объединенный
институт
ядерных
исследований
дубна



E7-84-85

P.Mädler

# ARE PROMPTLY EMITTED PARTICLES REALLY SEEN IN TDHF?

Submitted to "Zeitschrift für Physik A"

1984

## 1. INTRODUCTION AND MOTIVATION

One of the most salient features of heavy ion collisions is the emission of very fast light particles. It is believed that properties of such particles provide a source of information about early stages of the collisions, where thermal equilibrium is not yet established.

High-energy single nucleon spectra have been measured in coincidence with fusion-like /1,2/ as well as with deeply inelastic events/3/. These data have been analysed by different models considering either a locally equilibrated hot zone /4/, an equilibration process in the framework of slightly extended pre-equilibrium models originally developed for light-particle induced reactions/5,6/, or the so-called Fermi-jets or promptly emitted particles (PEP)/7,8/.

These approaches seem to give similar results with respect to inclusive data, even though they are based on quite different physical assumptions. The comparison with experimental data /2/ seemingly somewhat favours the modified Harp-Miller-Berne model /5/. However, in this framework angular distributions cannot be calculated, and the initial degree of freedom $n_0$ is not yet well understood quantitatively. Furthermore, it is by no means clear whether the disadvantages of the other models (say, the failure of the Fermi-jet model in predicting the high-energy component at large angles/2/) are a consequence of their underlying physical picture rather than an unsuitable realization of that picture through a number of ad hoc assumptions concerning geometry, dynamics, etc.

In this connection investigations of pre-equilibrium emission of light particles recently performed using the time-dependent Hartree--Fock (TDHF) approach/9,10,11/ are of great interest since given the effective nucleon-nucleon interaction the time evolution of the colliding system is determined by the basic equations /12,13,14/. In TDHF calculations PEP are identified with a low-density component (a few percent of the central nuclear density $\rho_0$) emerging in forward direction beyond the fragment wall at a typical time of an order of 1-2 times the transit time $t_{trans}$ (several $10^{-22}$ s) of a nucleon across the recipient nucleus and escaping with a velocity up to about twice the incident beam velocity.

Results of realistic TDHF studies reported in [9,10] for the $^{16}O + ^{93}Nb$ reaction semiquantitatively reproduce some main properties of the measured pre-equilibrium particles. This, for example, concerns multiplicities of fast particles or the threshold-like onset of their appearance at a center-of-mass energy per nucleon above the Coulomb barrier $(E_{c.m.}-V_0)/\mu$ around 5 MeV as well as an increase of fast-particle emission with increasing incident energy. Similar agreement with integral characteristics of the data can be achieved [2] by applying the Fermi-jet model[7]. In this approach it is basically assumed that a nucleon transferred from the donor nucleus to the recipient in the latter moves with a velocity that is simply the sum of its initial Fermi velocity and the velocity of relative motion of the colliding ions. Thus, TDHF seems to give arguments in favour of a strong coupling between Fermi and relative motion. This, in turn, would mean that the dynamics of the self-consistent mean field, leading, for example, to a rearrangement of the single-particle momentum distribution (compared to two Fermi spheres shifted by the velocity of relative motion), to some time dependence of the barrier between the ions which the nucleons tunnel through, etc., is negligible if looking for fast particle emission.

However, recently the TDHF equations have been solved for $\alpha + \alpha$ and $^{16}O + ^{16}O$ central collisions[15] at several incident energies by using an expansion of the single-particle wave functions in terms of static orthogonal basis functions constructed from orthogonal polynomials weighted with a two-center function. It was found that the maximum density $\rho_{max}$ of nucleonic jets rapidly decreases with an increasing size of the basis. An upper limit of $\rho_{max} \approx 4\cdot 10^{-4}\ fm^{-3}$ was found for the largest set of basis function considered. It has been concluded that relative and Fermi motion are coupled weakly.

In the present paper we perform a numerical-stability study of PEP production in one-dimensional slab collisions using a finite difference method. In Sect.2 it is shown that "spurious" PEP appear if numerical stability is not yet reached. Section 3 contains a systematic study of incident energy and mass dependence of "real" (i.e., numerically stable) PEP. Section 4 deals with a systematics of these results. A comparison with corresponding data from more realistic TDHF studies is made. This allows one to draw the conclusion that the Fermi-jet mechanism cannot be responsible for most of the energetic



nucleons seen in experiment. A smooth transition to fragmentation is indicated in Sects. 3 and 4.

## 2. MODEL AND NUMERICAL METHOD

In this work a numerical investigation of step size and box length effects upon PEP production is performed in the framework of a simple effectively one-dimensional model for slab collisions [12] in which the (frozen) Fermi motion in the directions perpendicular to the scattering axis is taken into account. It is known that this slab geometry qualitatively exhibits all essential features of realistic TDHF calculations including fast particle emission[12,13,14]. Furthermore, the real dynamics of the fast particle emission should preferentially proceed in one dimension since they are known to appear in near-central collisions and to be emitted in forward directions. Therefore, for a study of the numerical stability of PEP as well as for some semi-quantitative conclusions (order-of-magnitude estimates) this model should be a reasonable starting point.

The effective nucleon-nucleon interaction is chosen to be a simplified Skyrme force

$$V(\vec{r}_1,\vec{r}_2) = (t_0 + \frac{t_3}{6}\rho)\ \delta(\vec{r}_1 - \vec{r}_2) \qquad (1)$$

with $t_0=-1090$ MeV fm$^3$ and $t_3=17288$ MeV fm$^6$ and $\rho$ being the one-body density

$$\rho(\vec{r},t) = \rho(z,t) = \sum_{n=1}^{N} a_n\ |\phi_n(z,t)|^2 . \qquad (2)$$

The occupation numbers $a_n$ are smaller than unity (but constant in time) due to the Fermi motion in transverse directions which is decoupled from the motion parallel to the z-axis and described by plane waves. The TDHF equations

$$i\hbar\,\dot{\phi}_n(z,t) = \left[-\frac{\hbar^2}{2m}\frac{\partial^2}{\partial z^2} + \frac{3}{4}t_0\,\rho(z,t) + \frac{3}{16}t_3\,\rho^2(z,t)\right]\phi_n(z,t) \qquad (3)$$

for N single-particle wave functions $\phi_n(z,t)$ are solved numerically. Initial conditions are constructed from stationary solutions of (3) boosted together by plane waves (for details see [12]).

The numerical method used to solve (3) is a finite-series expansion of the evolution operator with the mean-field Hamiltonian h taken at half time step

$$\phi_n(t+\Delta t) \approx \exp\left[-\frac{i}{\hbar}\Delta t\cdot h(t+\frac{1}{2}\Delta t)\right]\phi_n(t)$$
$$\approx \sum_{j=0}^{J}\frac{1}{j!}\left[-\frac{i}{\hbar}\Delta t\cdot h(t+\frac{1}{2}\Delta t)\right]^j \phi_n(t) \qquad (4)$$

which is evaluated using a Horner scheme. We found a value of J=4 to be sufficient to obtain stable results in any calculation described below even for instants long after the emission of PEP. The spatial second derivative appearing in h is approximated by the five-point finite difference expression. The boundary conditions are that the wave functions $\phi_n$ vanish in the first and last pairs of grid points of the z-coordinate mesh (reflecting edges). Applying the equation of continuity at time t the time step $\Delta t$ for the following iteration is determined from the requirement that the relative change of density at any grid point should not exceed 1 per sent. So $\Delta t$ is not a constant during the calculation. For a grid-point spacing $\Delta z$=0.5 fm several hundred time steps are typical for the evolution in a time interval of the order of $t_{trans}$. In all calculations that we have performed a further decrease of $\Delta t$ did not yield any significant influence on the time evolution of the system. The step in coordinate space $\Delta z$ has been varied from 1 fm to 0.2 fm and the size of the numerical box L from 64 fm to 128 fm. In most cases numerical stability could be reached for $\Delta z \lesssim 0.5$ fm and L $\gtrsim$ 80–120 fm (depending somewhat on the incident energy and slab thickness). Norm and energy conservation have been proved to be fulfilled even for the largest step size z=1 fm to within 0.1% or less during the whole evolution process.

## 3. FROM SPURIOUS TO REAL PEP

We start discussion with collisions of symmetric thick slabs of slab thickness $A_1=A_2=2.0$ fm$^{-2}$ (compare with the slab-mass table in/12/).

For two different spatial step sizes (1 fm and 0.8 fm) the time evolution of the density profile for an incident energy of $(E/A)_{c.m.}$ = 4 MeV is shown in Fig.1 in comparison with a free translation of a single slab with the same initial velocity calculated with $\Delta z$=1 fm. It is seen that for $\Delta z$=1 fm fast PEP-like low-density components emerge which are exactly the same for the collision as well as for the free translation at t $\lesssim$ 50 fm/c. Thus, we obviously are dealing with an effect of numerical inaccuracy as a consequence of which matter is left behind the moving slab instead of being pushed through the collision partner. After passing the turning point of the collision both curves naturally diverge except the density ripples on the right which, as we shall see, are connected with the finite box size (L=64 fm in the given case). If the grid-point spacing is only slightly decreased to 0.8 fm, this type of "spurious" PEP immediately disappears,



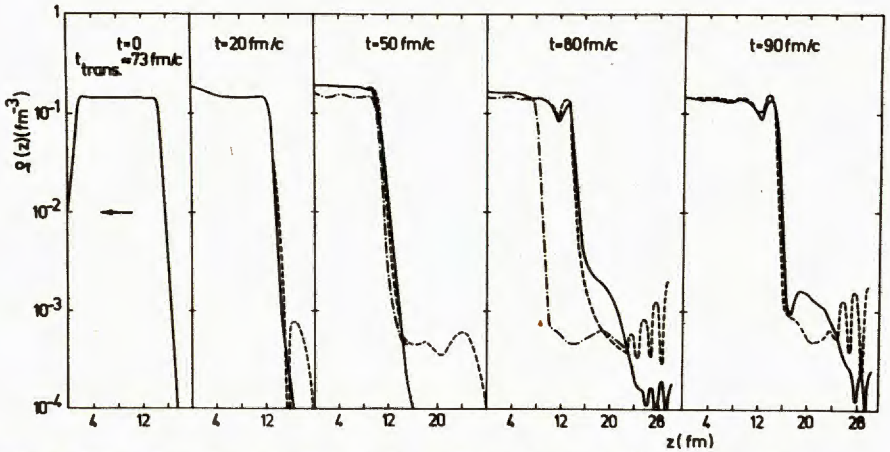


Fig.1. The time evolution of the nuclear density $\rho(z)$ for the symmetric $A_1=A_2=2.0$ fm$^{-2}$ slab collision at $(E/A)_{c.m.}$=4 MeV in a numerical box of L=64 fm, for $\Delta z$=1 fm (dashed lines) and $\Delta z$=0.8 fm (full lines) as well as for a free translation calculated with $\Delta z$=1 fm (dashed-dotted lines).

and the "real" PEP begin to emerge at t=80 fm/c comparable with $t_{trans}$. Note that this jet of nucleonic matter is not seen at all for the larger value of $\Delta z$. With a further decrease of $\Delta z$ and a larger value of L=100 fm its shape becomes stable at about $\Delta z$=0.4 fm and takes the form shown in fig.2 (full line). With the same value of $\Delta z$ but in the smaller box of fig.1 the real PEP at times t > 80 fm/c get increasingly deformed (dashed line in fig.2) so that the density profiles seem to indicate a subsequent emission of several quite small in thickness (1-3 fm) nucleonic jets with central densities rapidly increasing with decreasing box size and increasing with time. The real jet, however, in its further time evolution becomes broader and broader and, correspondingly, decreases in its central density. In any case these diffraction-like deformations of the stable jet shape emerge long before the essential part of the PEP is reflected by the edges of the box. It has been found that they begin to develop at a typical time when the $\rho=10^{-5}$ fm$^{-3}$ density end of the jet reaches the edge of the box. This is about 80 fm/c for L=64 fm in fig.2 and 150 fm/c for L=100 fm (not seen in fig.2). So, a clean separation of PEP from the target can be reached only for sufficiently large L ( L $\gtrsim$ 100 fm in the given case) and sufficiently small $\Delta z$( $\lesssim$ 0.4 fm here).

Fig.2. The time evolution of the same system as in fig.1 using $\Delta z$=0.4 fm, L=64 (dashed lines) and L=100 fm (full lines). Only the edge of the fragment in the right half of the box and the low-density tail is shown.

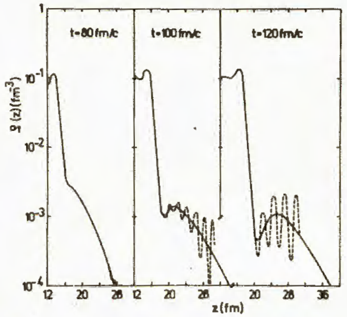


In the light of the above statements we suspect that the multiplicities of PEP in the realistic calculations of [9,10] are to some extent overestimated. In these papers box sizes of L=34 fm [9] and L=44 fm[10] have been used. The corresponding values of $\Delta z$, unfortunately, are not explicitly given. On the other hand, we claim that the rapid decrease of nucleonic jets with increasing number of basis functions found in[16] and their multi-humped shapes, resembling those of our fig.1, express nothing else but the presence and step by step elimination of spurious PEP connected with the specific method of[16]. Probably, a further enlargement of their basis would lead to stable PEP. However, it seems to us that the time-independent two-centered basis used in [16] is possibly very useful if looking for the evolution of the two fragments only but quite unsuitable and slow-convergent with respect to fast low-density objects emerging and propagating far from the two centers.

## 4. ENERGY AND MASS DEPENDENCE

We turn now to the discussion of the incident energy and slab-thickness dependence of PEP emission.

In fig.3 the time evolution of the density profile of the $A_1=A_2$= 2.0 fm$^{-2}$ system is shown for an incident energy $(E/A)_{c.m.}$=1.5 MeV. The influence of the box edges is removed by choosing L=120 fm.

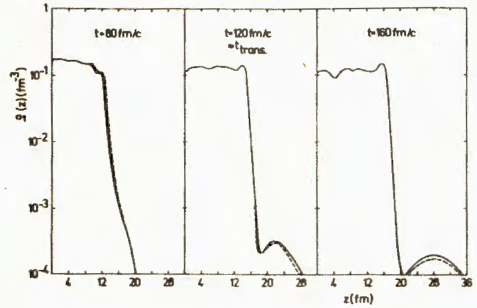


Fig.3. The time evolution of $\rho(z)$ for the $(E/A)_{c.m.}$= 1.5 MeV, $A_1=A_2$=2.0 fm$^{-2}$ collision with L=120 fm, $\Delta z$=0.8 fm (dashed lines) and $\Delta z$=0.5 fm (full lines)



Note that in going from the profiles calculated with $\Delta z$=0.8 fm to the numerically stable shape, reached for $\Delta z$=0.5 fm, the central density $\rho_{max}$ of the PEP still somewhat increases. This is a similar situation as in fig.1 and opposite to the finding of[16] for increasing the basis. At this small energy the central density of the separated jet amounts only to about $\rho_{max}=2\cdot10^{-4}$ fm$^{-3}$.

For higher incident energies $\rho_{max}$ and correspondingly the number of nucleons in the jet $\Delta A$ increases. If in the case of $(E/A)_{c.m.}$ =4 MeV (fig.2) $\rho_{max}\approx10^{-3}$ fm$^{-3}$, for the $(E/A)_{c.m.}$= 8 MeV collision it amounts to about $4\cdot10^{-3}$ fm$^{-3}$. The latter case is illustrated in fig.4. It is interesting from several points of view. First it is remarkable that the nucleon jet has a very broad velocity distribution and begins to separate into two components at about t=120 fm/c. This can be seen from the very flat fall-off of the density in front of the much steeper one around the small density maximum at z=26 fm. Since the further evolution of the faster jet component exhibiting a mean velocity of 1.5 times the projectile velocity $v_0$ is connected with a rapid broadening in space, we could not achieve its clean separation from the larger but slower component (moving with a mean velocity of about $v_0$) in the given large box of L=130 fm before its shape becomes increasingly deformed. So, we approximately determined its characteristics ( $\rho_{max}$, $\Delta A$ and mean velocity) by substracting the extrapolated shape of the slower component from the total shape at two instants (120 and 140 fm/c) in both cases finding nearly the same estimates. A qualitatively similar result of the appearance of a small fast and a larger but slower nucleonic jet was also obtained in a realistic treatment of a near central $^{12}C+^{197}Au$ reaction at $(E/A)_{Lab}$=30 MeV incident energy[11].

A second interesting point in the evolution shown in Fig.4 is that at t $\approx$ 90 fm/c a small lump of central nuclear density seems to separate. However, at a later instant it is trapped back by the

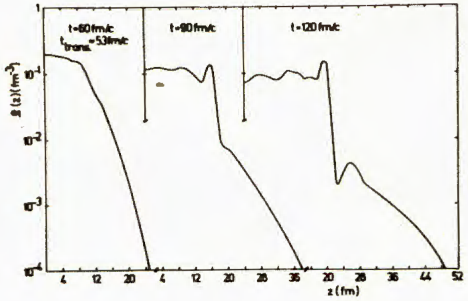


**Fig.4. The time evolution of $\rho$ (z) for the $(E/A)_{c.m.}$= =8 MeV, $A_1=A_2$=2.0 fm$^{-2}$ collision with L=130 fm, $\Delta z$= =0.4 fm.**

Fig.5. The time evolution of $\rho(z)$ for the $(E/A)_{c.m.}$ = =15 MeV, $A_1$=$A_2$= =2.0 $fm^{-2}$ collision with L=64 fm, $\Delta z$= =0.8 fm (dashed lines) and L=100 fm, $\Delta z$=0.3 fm (full lines).

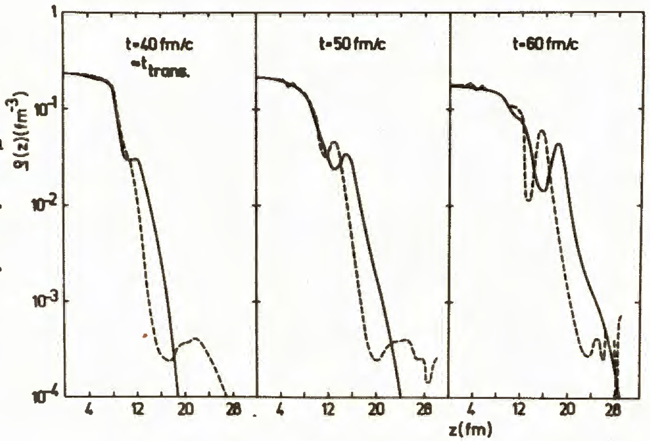


main fragments flying apart at this time. Therefore, the $(E/A)_{c.m.}$ = = 8 MeV case for $A_1$ = $A_2$ = 2.0 $fm^{-2}$ in some sense seems to be transitional between binary processes and fragmentation, both accompanied by fast nucleon emission.

To confirm this, in fig.5 the evolution of the colliding slabs at $(E/A)_{c.m.}$=15 MeV is shown. It can be seen that besides the quasi-free fast jet component beginning to emerge at about t=60 fm/c, $\rho_{max}$=$10^{-3}$ $fm^{-3}$ (not yet separated in fig.5) a much larger but slower jet moving about $v_0$ appears similar as in the previous case. However, this time its central density of already about 0.04 $fm^{-3}$ at $t \approx t_{trans}$ grows up to nearly $\rho_0$ . Thus, we are dealing with a fragmentation + PEP emission process. To give an imagination of the step and box size effects at this high incident energy in fig.5 calculations for $\Delta z$=0.8 fm, L=64 fm and $\Delta z$=0.3 fm, L=100 fm (stable shape) are shown. Both kinds of spurious PEP discussed above as well as the appearance of the real PEP only for a sufficiently high accuracy are clearly seen.

At a still higher incident energy of $(E/A)_{c.m.}$= 25 MeV a further calculation for the $A_1$=$A_2$=2.0 $fm^{-2}$ system has been performed in a very large box of L=200 fm and a step size of $\Delta z$=0.3 fm (fig.6). The time evolution of the system was followed up to t=200 fm/c $\approx 7 \cdot t_{trans}$. In this case the first fragment begins to grow out of a $\rho \approx 0.05$ $fm^{-3}$ lump appearing in front of the slabs at about $t$=$t_{trans} \approx 30$ fm/c similar as in the 15 MeV case. However, at this higher energy, after separating, it moves with a velocity $v_1 \approx 1.7\ v_0$, i.e., is nearly as fast as the low-density fast nucleon jet (which is not seen in fig.6). This confirms the result of [12] that after the onset of fragmentation of



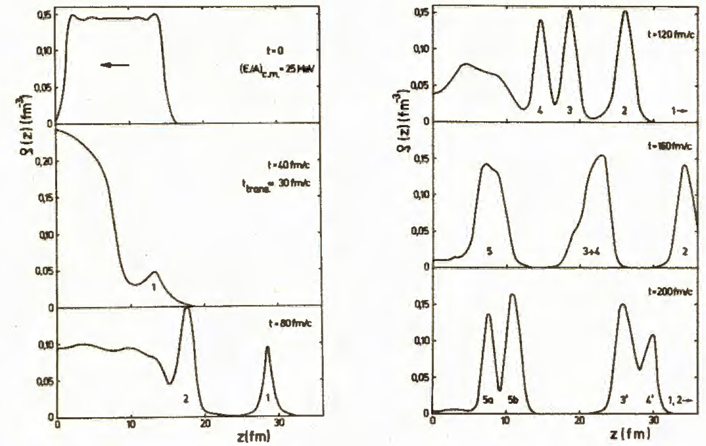


Fig.6. The time evolution of $\rho(z)$ for the $(E/A)_{c.m.}$=25 MeV, $A_1$=$A_2$= =2.0 $fm^{-2}$ collision with L=200 fm, $\Delta z$=0.3 fm in a linear scale for the density. Only part of the right half box is shown.

further increase of incident energy is needed to get a leading fragment substantially faster than the projectile. The second fragment emerging at about $t$=$2 \cdot t_{trans}$ has still a very high velocity of $v_2$=0.9 $v_0$. In the course of the collision process both slabs are totally fragmented into six fragments each. Concerning the fast nucleonic jet we established that it begins to appear at about t=60 fm/c in front of the first fragment. Due to their quite close mean velocities the jet does not really separate from the fastest fragment but quickly broadens in space. So at t=120 fm/c $\approx 4 \cdot t_{trans}$ the central jet density is $\rho_{max}$= $1.38 \cdot 10^{-3}$ $fm^{-3}$ at position z =±52 fm, while the minimum density between the fragment and the jet is $\rho_{min}$= = $1.19 \cdot 10^{-3}$ $fm^{-3}$ at position z=±48 fm. At this time, in a region up to z=±70 fm, the jet density is larger than $10^{-4}$ $fm^{-3}$. Later on the jet is melting away and starting to interact with the edges of the box.

To get an impression of the mass (slab thickness) dependence, calculations have been performed for $A_1$=$A_2$=0.75 $fm^{-2}$ collisions at incident energies $(E/A)_{c.m.}$=1.5,5,10 MeV. The corresponding density profiles at some typical instants are shown in Fig.7. A comparison with previous cases at comparable energies indicates an increase of the PEP intensity with $A_1$ as could be expected from phase space considerations. Obviously for light symmetrical collisions the on-

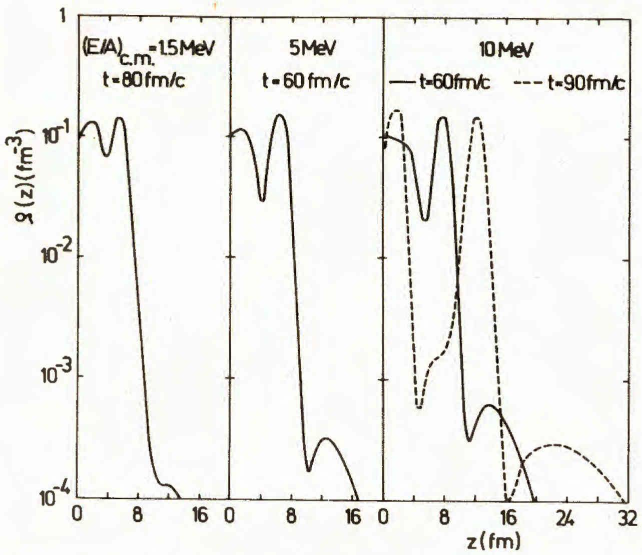


Fig.7. Density profiles of $A_1=A_2=0.75$ fm$^{-2}$ collisions, at several incident energies, shown at some typical instants.

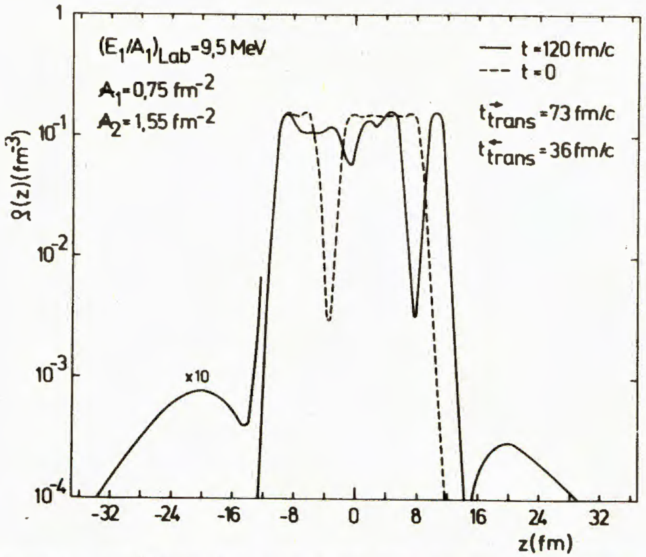


Fig.8. Density profiles for the slab collision simulating the $^{16}O+^{93}Nb$ reaction at incident energy $E_{Lab}$=204 MeV.



set of fragmentation lies lower in energy than for the heavy systems. In the given case already the 5 MeV collision leads to a single fast ($v_1 \approx v_0$) fragment on each side while the remaining system fuses. Naturally the number of fragments is smaller for the light systems than for heavy ones.

As a typical case for asymmetric slab collisions we have chosen the $A_1$=0.75 fm$^{-2}$, $A_2$=1.55 fm$^{-2}$, $(E/A)_{Lab}$=9.5 MeV system. This example to some extent is our one-dimensional analog of the $^{16}O+^{93}Nb$ reaction at $E_{Lab}$=204 MeV (investigated in /9,10/) with respect to the slab diameter as well as the energy per nucleon above the Coulomb barrier ($V_C$=0 in our calculations). Fig.8. shows the density profiles at contact time (t=0) and at t=120 fm/c when on both sides fast nucleonic jets begin to separate. The ratio of the number of fast nucleons originating from the projectile to those coming from the target amounts to $\Delta A_1 : \Delta A_2$ = 3.4.

## 5. SYSTEMATICS AND CONCLUSIONS

We return now to the discussion of the contradictorily results of /9,10/ and /15/ concerning the PEP intensity, i.e., the question to what extent a supposed direct coupling between Fermi and relative motion /7,8/ is weakened in a TDHF evolution. For this aim in figs. 9 and 10 the central density $\rho_{max}$ of the nucleonic jet and the number of nucleons in the jet divided by the mass number of the donor fragment $\Delta A/A$ are plotted against the incident energy per nucleon above the Coulomb barrier $(E_{c.m.} - V_C)/\mu$ (for $V_C$=0, as in our case, this quantity is equal to $(E/A_p)_{Lab}$= $(E/A)_{c.m.}(A_p+A_t)^2/(A_pA_t)$ with p and t standing for projectile and target, correspondingly, and for our symmetric slab collisions it is simply $4(E/A)_{c.m.}$). All slab collisions described above as well as results of more realistic TDHF studies /9,10,11,15/ are included.

Besides a general nearly linear increase of $\rho_{max}$ and $\Delta A/A$ with increasing energy an A dependence stronger than $\Delta A \sim A$ can be deduced from Fig.10 (comp., e.g., crosses and stars). Since in a simple Fermi gas picture /16/, for mass symmetric collisions at a fixed relative velocity, the relative amount $\Delta A/A$ of nucleons fulfilling the escape condition should be constant for varying A, one can conclude that the coupling between Fermi and relative motion in a TDHF evolution becomes the weaker the smaller the system is. A similar conclusion can also be drawn from comparing the $\alpha + \alpha$ with the $^{16}O+^{16}O$ results for $\rho_{max}$ /15/ since this quantity behaves similar to $\Delta A/A$.

When looking for the asymmetric $A_1$=0.75 fm$^{-2}$, $A_2$=1.55 fm$^{-2}$ slab collision it is seen that the amount $\Delta A/A$ of PEP originating from the light projectile is substantially higher (by a factor of about 4) than it would be in the corresponding light symmetric $A_1=A_2$=0.75 fm$^{-2}$ system at the same incident energy. This, to some extent, can be explained by the fact that in the asymmetric collision a larger amount of the incident energy is available for relative motion, i.e., due to the energy dependence stated above a larger value of $\Delta A/A$ results. By similar arguments it becomes clear that the PEP from the heavy target are somewhat suppressed compared to the $\Delta A/A$ value for $A_1=A_2$=1.55 fm$^{-2}$ collisions at the same incident energy (not shown here but presumably lying in between the values for the two investigated symmetric systems).

Due to this asymmetry effect it seems to be evident that the value of $\rho_{max}$ for a $^{12}$C+$^{12}$C collision in a realistic TDHF calculation would be substantially smaller than that of the quasifree nucleonic jet in the $^{12}$C+$^{197}$Au reaction /11/ at the same incident energy per nucleon. Therefore, since the diameter of the A=0.75 fm$^{-2}$ slab is close to that of a $^{12}$C nucleus, from a comparison with the values of $\rho_{max}$ for our light symmetric system, it follows that in realistic TDHF calculations less PEP emerge than in the corresponding one-

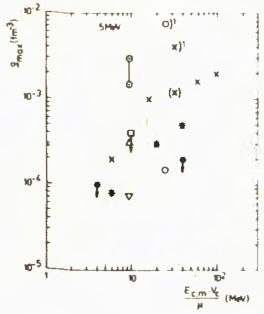

Fig.9. The central density $\rho_{max}$ of the fast nucleonic jet for several collisions plotted against the center-of-mass energy per nucleon above the Coulomb barrier: ✕ - symmetric $A_1$ = = $A_2$ = 2.0 fm$^{-2}$ slab collision (present work), ✱ - symmetric $A_1$ = $A_2$ = 0.75 fm$^{-2}$ slab collision (present work), △ , ▽ - nucleonic jet originating from the $A_1$ = 0.75 fm$^{-2}$ projectile, from the $A_2$ = 1.55 fm$^{-2}$ target in the asymmetric slab collision shown in Fig.8, ● - central $\alpha+\alpha$ collisions /15/, □ - central $^{16}$O + $^{16}$O collisions /15/, ○ - near central (L = 12$\hbar$) $^{12}$C + $^{197}$Au collision /11/, ◉ - $^{16}$O + $^{93}$Nb collision (L = 0) (the region "1-2% of the central nuclear density" quoted in /9/ is indicated by two corresponding marks). ↓ has the meaning "upper limit". In two cases besides the point for the PEP a second one of the same kind (marked ...)$^{1)}$ is plotted which corresponds to a second jet with velocity $v_2 \lesssim v_0$. The point in brackets results from fig.4 by extrapolation (see text to fig.4). The vertical dashed line marks that energy above which substantional amounts of fast particles have been seen in experiment /2/.



-dimensional evolution. This, in turn, is in agreement with the statement of /15/ that their values of $\rho_{max}$ are only upper limits.

If so, the results of /9,10/ for the $^{16}$O+$^{93}$Nb reaction are substantially overestimated, since they predict even more PEP than in our corresponding one-dimensional slab collision by nearly an order of magnitude (see both figs.9 and 10). Possible reasons for this have been discussed in Sect.3.

Hence, our main result of the present investigation is that the Fermi to relative motion coupling in a TDHF evolution is really very weak. To give an impression of the degree of weakening this coupling in TDHF for the $^{16}$O+$^{93}$Nb system the result of a simple Fermi gas estimate assuming ideal strong coupling (for details see /16/) is included in fig.10. This curve is not normalized as it has been done in /9,10,11/.

As indicated in Sect.4 the transition to fragmentation proceeds in a quite smooth way. For the $A_1=A_2$=2.0 fm$^{-2}$ slab collision this is illustrated in fig.10. The lower branch of the line connecting the calculated points to guide the eye corresponds to the quasi-free jet (PEP) with $v \gtrsim v_0+v_F$ . Above $(E/A)_{c.m.} \approx$ 5 MeV a second low-density nucleonic jet with $v \lesssim v_0$ emerge which in its further evolution broadens and decreases in $\rho_{max}$ as the quasi-free jet does, since there is no binding at such low densities. Our $(E/A)_{c.m.}$=8 MeV ($E_{c.m.}/\mu$ =32 MeV) case, resembling the result of /11/ (see fig.9), is typical for such a situation and gives a point on the second

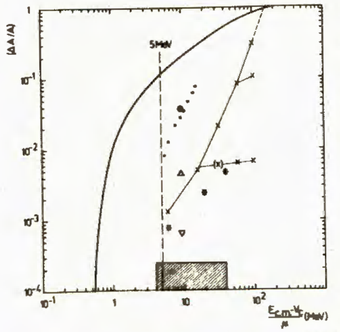

Fig.10. The number of nucleons in the jet divided by the number of nucleons in the donor nucleus $\Delta A/A$ as a function of incident energy. The marks have the same meaning as in fig.9. The additional series of points is for central $^{16}$O + $^{93}$Nb collisions and taken from /10/. Since no precise values $\Delta A/A$ are given in /15/, only a hatched region is shown defined by the energy range considered in /15/ and by an upper limit of $\Delta A/A = 2.5 \cdot 10^{-4}$ quoted therein. For the $^{12}$C + $^{197}$Au reaction no value of $\Delta A/A$ could be deduced from /11/. For $A_1$ = $A_2$ = 2.0 fm$^{-2}$ slab collisions all jets and fragments exhibiting velocities $v \gtrsim$ 0.9 v are included. The thick full line is a simple Fermi gas estimate for the $^{16}$O + $^{93}$Nb system.

branch of the line in fig.10. At some higher energy this second jet developes into a first fragment of still $v \approx v_0$. Above $(E/A)_{c.m.}$ = = 15 MeV a second fragment (third branch) with $v_2 \approx v_0$ appears and the first one acquires a velocity close to the mean PEP velocity (compare our $(E/A)_{c.m.}$ = 25 MeV collision). It is interesting to mention that a formal extrapolation to still higher energies comes close to the Fermi gas estimate, i.e., all fragments would have velocities close to or larger than $v_0$.

Since residual two-body interactions, not included in standard TDHF, are expected to have an increasing influence on the dynamics of the collision process, our results concerning fragmentation surely are of minor physical relevance.

On the basis of our result that a TDHF evolution should exhibit substantially less PEP than predicted in /9,10/ in semi-quantitative agreement with experimental data, we conclude that the Fermi-jet mechanism is not responsible for most of the fast particles emerging in heavy-ion collisions. Hence, in any case, two-body correlations have to be taken into account. Certainly short-range nucleon-nucleon interactions, for which some kinematically allowed final states are no longer blocked by the Pauli principle, can play an essential role in this connection /14,17/ . Long-range residual interactions if, as usually, treated in the Markov approximation drive the system towards thermal equilibrium and should, in turn, further decrease the PEP mechanism. In this connection investigations of coherent multiparticle phenomena caused by the residual interaction would be of great interest.

A final remark concerns the ability of TDHF to explain even that small fraction of energetic nucleons which possibly underlies the PEP mechanism. It is known /14/ that additional high-momentum components appear in a TDHF evolution, which are generated by the motion of the surfaces of the mean field. The latter is determined by the effective nucleon-nucleon force which itself is only adopted for bulk properties of static nuclei and nuclear matter. To the extent to which this type of high-momentum components form the PEP and to which a (still unknonw) effective nucleon-nucleon force to be used in dynamic calculations at high excitations differs from, say, the standard Skyrme forces, these PEP could be basically spurious even in a numerical stable calculation.

The author is grateful to J.A.Maruhn for kindly providing him with a one-dimensional TDHF computer code which was only slightly modified to perform the calculations presented in this paper. A useful discussion on numerical details is also acknowledged.



REFERENCES

1. Britt H.C., Quinton A.R. Phys.Rev., 1961, 124, p.877;
Gallin J. et al. Phys.Rev., 1974, C9, p.1126;
Westberg L. et al. Phys.Rev., 1978, C18, p.796.
2. Holub E. et al. Phys.Rev., 1983, C28, p.252.
3. Gauron A. et al. Phys.Rev.Lett., 1981, 46, p.8.
4. Weiner R., Weström M. Phys.Rev.Lett., 1975, 34, p.1523;
Morrison W.W. et al. Phys.Lett., 1980, 93B, p.379;
Garpman S.I.A., Sperber D., Zielinska-Pfabe M. Phys.Lett, 1980, 90B, p.53.
5. Blann M. Phys.Rev., 1981, C23, p.205.
6. Yoshida S. Z.Phys., 1982, A308, p.133.
7. Bondorf J.P. et al. Phys.Lett., 1979, 84B, p.163;
Bondorf J.P. et al. Nucl.Phys., 1980, A333, p.285.
8. Sebille F., Remaud B. Z.Phys., 1983, A310, p.99.
9. Devi K.R.S. et al. Phys.Rev., 1981, C24, p.2521.
10. Dhar A.K. et al. Phys.Rev., 1982, C25, p.1432.
11. Stöcker H. et al. Phys.Lett., 1981, 101B, p.379.
12. Bonche P., Koonin S.E., Negele J.W. Phys.Rev., 1976, C13, p.1226.
13. Negele J.W. In: Theoretical Methods in Medium Energy and Heavy Ion Physics. Eds. McVoy K., Friedman W., Plenum Press, N.Y., p.235.
14. Negele J.W. Rev.Mod.Phys., 1982, 54, p.913.
15. Drozdz S., Okolowicz J., Ploszajczak M. Phys.Lett., 1983, 121B, p.297.
16. Davies K.T.R. et.al. Preprint MAP-23, 1982.
17. Mädler P. Nucl.Phys., 1983, A404, p.58.

Received by Publishing Department
on February 10,1984

## WILL YOU FILL BLANK SPACES IN YOUR LIBRARY?

**You can receive by post the books listed below. Prices - in US $, including the packing and registered postage**

| | | |
|---|---|---|
| D4-80-385 | The Proceedings of the International School on Nuclear Structure. Alushta, 1980. | 10.00 |
| | Proceedings of the VII All-Union Conference on Charged Particle Accelerators. Dubna, 1980. 2 volumes. | 25.00 |
| D4-80-572 | N.N.Kolesnikov et al. "The Energies and Half-Lives for the $\alpha$ - and $\beta$-Decays of Transfermium Elements" | 10.00 |
| D2-81-543 | Proceedings of the VI International Conference on the Problems of Quantum Field Theory. Alushta, 1981 | 9.50 |
| D10,11-81-622 | Proceedings of the International Meeting on Problems of Mathematical Simulation in Nuclear Physics Researches. Dubna, 1980 | 9.00 |
| D1,2-81-728 | Proceedings of the VI International Seminar on High Energy Physics Problems. Dubna, 1981. | 9.50 |
| D17-81-758 | Proceedings of the II International Symposium on Selected Problems in Statistical Mechanics. Dubna, 1981. | 15.50 |
| D1,2-82-27 | Proceedings of the International Symposium on Polarization Phenomena in High Energy Physics. Dubna, 1981. | 9.00 |
| D2-82-568 | Proceedings of the Meeting on Investigations in the Field of Relativistic Nuclear Physics. Dubna, 1982 | 7.50 |
| D9-82-664 | Proceedings of the Symposium on the Problems of Collective Methods of Acceleration. Dubna, 1982 | 9.20 |
| D3,4-82-704 | Proceedings of the IV International School on Neutron Physics. Dubna, 1982 | 12.00 |
| D2,4-83-179 | Proceedings of the XV International School on High-Energy Physics for Young Scientists. Dubna, 1982 | 10.00 |
| | Proceedings of the VIII All-Union Conference on Charged Particle Accelerators. Protvino, 1982. 2 volumes. | 25.00 |
| D11-83-511 | Proceedings of the Conference on Systems and Techniques of Analitical Computing and Their Applications in Theoretical Physics. Dubna,1982. | 9.50 |
| D7-83-644 | Proceedings of the International School-Seminar on Heavy Ion Physics. Alushta, 1983. | 11.30 |
| D2,13-83-689 | Proceedings of the Workshop on Radiation Problems and Gravitational Wave Detection. Dubna, 1983. | 6.00 |

Orders for the above-mentioned books can be sent at the address:
Publishing Department, JINR
Head Post Office, P.O.Box 79 101000 Moscow, USSR

Мэдлер П. E7-84-85

Дает ли зависящий от времени метод Хартри-Фока мгновенно испущенные частицы?

Проводится систематическое исследование численной стабильности испускания быстрых нуклонных струй малой плотности в одномерных столкновениях ядерных слоев. Показано, что ложные струи связаны или со слишком большим пространственным шагом или со слишком узкой пространственной областью интегрирования. Систематика полученных результатов и сравнение с более реалистическими, но несколько противоречивыми, расчетами по методу Хартри-Фока с зависимостью от времени /ЗВХФ/ позволяет заключить, что связь внутреннего и относительного движения в эволюции по ЗВХФ очень слабая и что механизм фермиевских струй не может отвечать за большинство энергетических нуклонов, обнаруженных в эксперименте. Исследуется переход к фрагментации.

Работа выполнена в Лаборатории теоретической физики ОИЯИ.

Препринт Объединенного института ядерных исследований. Дубна 1984

Mädler P. E7-84-85

Are Promptly Emitted Particles Really Seen in TDHF?

A systematic study of numerical stability of the emission of fast low-density nucleonic jets in one-dimensional slab collisions is performed. Spurious jets are shown to be connected with either a too large grid-point spacing or with a too small numerical box. From a systematics of our results and comparison with fast-particle predictions in more realistic, but somewhat contradictorily TDHF studies it is concluded that the coupling of the intrinsic motion to the relative motion in a TDHF evolution is very weak so that the Fermi-jet mechanism cannot be responsible for most of the energetic nucleons observed in experiment. The transition to fragmentation is investigated.

The investigation has been performed at the Laboratory of Theoretical Physics, JINR.

Preprint of the Joint Institute for Nuclear Research. Dubna 1984